Acta Crystallographica Section B
Structural Science
ISSN 0108-7681

3,5-Dihalo-4-hydroxybenzonitriles: isostructures, polymorphs and solvates

Doyle Britton

Department of Chemistry, University of Minnesota, Minneapolis, MN 55455-0431, USA

Correspondence e-mail: britton@chem.umn.edu

Received 29 April 2005
Accepted 19 November 2005

3,5-Dichloro-4-hydroxybenzonitrile and its solvates with benzene and xylene assemble in chain-like arrangements held together by OH···NC interactions. Two polymorphs each of the corresponding dibromo and diiodo compounds form similar chains which are then bound together by $X\cdots X$ interactions to form approximately planar sheets. These sheets are essentially identical in all four of the bromo and iodo compounds and have approximate *p2gg* two-dimensional symmetry. These four compounds form an extreme example of two-dimensional isostructuality. The polymorphs differ in the stacking arrangements. One of the Br polymorphs is isostructural with one of the I polymorphs.

1. Introduction

Baughman *et al.* (1981) determined the structure of bromoxynil, $Br_2C_6(OH)(CN)$, abbreviated as MBr, and found two crystallographically independent molecules in a triclinic unit cell. They noted that these two molecules were very close to being co-planar. Britton (2000) pointed out that this coplanarity extended to layers with a two-dimensional arrangement that could be described as being approximately in the plane group *p2gg*. This study compares the structures of the corresponding chloride, MCl, and iodide, MI, as well as a second polymorph of MBr.

The present report includes the structures of MCl, solvates of MCl with benzene and *p*-xylene, MCl-Bz and MCl-Xy, a redetermination of the previously reported MBr, now MBr-*A*, a second polymorph, MBr-*B*, and two polymorphs of MI, MI-*A* and MI-*C*. MI-*A* is isostructural with MBr-*A*. The second polymorph of MI is labelled MI-*C* to emphasize that it is not isostructural with MBr-*A*.

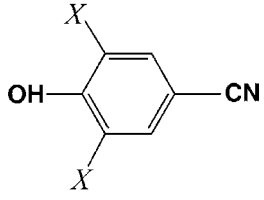

X = Cl		MCl
X = Cl	benzene solvate	MCl-Bz
X = Cl	xylene solvate	MCl-Xy
X = Br	two polymorphs	MBr-*A*, MBr-*B*
X = I	two polymorphs	MI-*A*, MI-*C*

Table 1
Experimental details.

	MCl	MCl-Bz	MCl-Xy	MBr-*A*
Crystal data				
Chemical formula	$C_7H_3Cl_2NO$	$C_7H_3Cl_2NO\cdot0.5C_6H_6$	$C_7H_3Cl_2NO\cdot0.25C_8H_{10}$	$C_7H_3Br_2NO$
M_r	188.00	227.06	214.55	276.92
Cell setting, space group	Triclinic, $P\overline{1}$	Triclinic, $P\overline{1}$	Monoclinic, $P2_1/n$	Triclinic, $P\overline{1}$
a, b, c (Å)	7.3325 (18), 8.999 (2), 12.221 (3)	7.420 (2), 8.386 (2), 8.808 (2)	4.5522 (11), 15.067 (4), 13.636 (3)	8.244 (2), 9.120 (2), 11.687 (3)
α, β, γ (°)	78.65 (1), 74.39 (1), 74.23 (1)	73.820 (10), 66.990 (10), 79.040 (10)	90.00, 98.00 (1), 90.00	95.60 (1), 108.55 (1), 106.13 (1)
V (Å^3)	740.7 (3)	482.4 (2)	926.2 (4)	783.4 (3)
Z	4	2	4	4
D_x (Mg m^{-3})	1.686	1.563	1.539	2.348
Radiation type	Mo $K\alpha$	Mo $K\alpha$	Mo $K\alpha$	Mo $K\alpha$
No. of reflections for cell parameters	1913	2490	3547	2861
θ range (°)	2.8–25.9	2.6–27.5	2.7–27.2	2.4–27.5
μ (mm^{-1})	0.81	0.63	0.65	10.28
Temperature (K)	174 (2)	174 (2)	174 (2)	174 (2)
Crystal form, color	Plate, colorless	Prism, colorless	Needle, colorless	Prism, colorless
Crystal size (mm)	0.40 × 0.25 × 0.10	0.50 × 0.45 × 0.40	0.40 × 0.15 × 0.10	0.20 × 0.15 × 0.15
Data collection				
Diffractometer	Siemens area detector	Siemens area detector	Siemens area detector	Siemens area detector
Data collection method	ω scans	ω scans	ω scans	ω scans
Absorption correction	Multi-scan (based on symmetry-related measurements)	Multi-scan (based on symmetry-related measurements)	Multi-scan (based on symmetry-related measurements)	Multi-scan (based on symmetry-related measurements)
T_{min}	0.80	0.74	0.88	0.174
T_{max}	0.92	0.78	0.94	0.214
No. of measured, independent and observed reflections	8796, 3362, 2309	5442, 2141, 2086	8934, 1636, 1317	9376, 3568, 3107
Criterion for observed reflections	$I > 2\sigma(I)$	$I > 2\sigma(I)$	$I > 2\sigma(I)$	$I > 2\sigma(I)$
R_{int}	0.054	0.015	0.054	0.027
θ_{max} (°)	27.5	0.015	0.054	0.027
Range of h, k, l	$-9 \Rightarrow h \Rightarrow 9$ $-11 \Rightarrow k \Rightarrow 11$ $-15 \Rightarrow l \Rightarrow 15$	$-9 \Rightarrow h \Rightarrow 9$ $-10 \Rightarrow k \Rightarrow 10$ $-11 \Rightarrow l \Rightarrow 11$	$-5 \Rightarrow h \Rightarrow 5$ $-17 \Rightarrow k \Rightarrow 17$ $-16 \Rightarrow l \Rightarrow 16$	$-10 \Rightarrow h \Rightarrow 10$ $-11 \Rightarrow k \Rightarrow 11$ $-15 \Rightarrow l \Rightarrow 15$
Refinement				
Refinement on	F^2	F^2	F^2	F^2
$R[F^2 > 2\sigma(F^2)]$, $wR(F^2)$, S	0.040, 0.095, 1.05	0.025, 0.075, 1.08	0.048, 0.079, 1.22	0.035, 0.079, 1.09
No. of reflections	3362	2141	1636	3568
No. of parameters	199	148	151	200
H-atom treatment	Constrained to parent site	Constrained to parent site	Constrained to parent site	Constrained to parent site
Weighting scheme	$w = 1/[\sigma^2(F_o^2) + (0.029P)^2 + 0.054P]$, where $P = (F_o^2 + 2F_c^2)/3$	$w = 1/[\sigma^2(F_o^2) + (0.039P)^2 + 0.211P]$, where $P = (F_o^2 + 2F_c^2)/3$	$w = 1/[\sigma^2(F_o^2) + (0.022P)^2 + 0.43P]$, where $P = (F_o^2 + 2F_c^2)/3$	$w = 1/[\sigma^2(F_o^2) + (0.028P)^2 + 2.2P]$, where $P = (F_o^2 + 2F_c^2)/3$
$(\Delta/\sigma)_{max}$	0.003	0.013	0.023	0.006
$\Delta\rho_{max}$, $\Delta\rho_{min}$ (e Å^{-3})	0.34, −0.28	0.46, −0.18	0.22, −0.19	0.65, −0.61
Extinction method	None	*SHELXTL*	*SHELXTL*	*SHELXTL*
Extinction coefficient	–	0.022 (4)	0.0043 (16)	0.0029 (3)

	MBr-*B*	MI-*A*	MI-*C*
Crystal data			
Chemical formula	$C_7H_3Br_2NO$	$C_7H_3I_2NO$	$C_7H_3I_2NO$
M_r	276.92	370.90	370.90
Cell setting, space group	Triclinic, $P\overline{1}$	Triclinic, $P\overline{1}$	Monoclinic, $P2_1/n$
a, b, c (Å)	3.9684 (10), 12.669 (3), 16.047 (4)	8.648 (2), 9.393 (2), 12.120 (2)	15.667 (4), 14.320 (4), 7.724 (2)
α, β, γ (°)	79.68 (1), 83.71 (1), 83.06 (1)	97.32 (1), 109.86 (1), 105.59 (1)	90.00, 91.90 (1), 90.00
V (Å^3)	784.7 (3)	865.5 (3)	1730.8 (8)
Z	4	4	8
D_x (Mg m^{-3})	2.344	2.846	2.841
Radiation type	Mo $K\alpha$	Mo $K\alpha$	Mo $K\alpha$
No. of reflections for cell parameters	2619	2025	3574
θ range (°)	2.8–27.2	2.6–27.5	2.6–27.5
μ (mm^{-1})	10.26	7.21	7.21
Temperature (K)	174 (2)	174 (2)	173 (2)
Crystal form, color	Plate, colorless	Prism, colorless	Needle, colorless

Table 1 (continued)

	MBr-*B*	MI-*A*	MI-*C*
Crystal size (mm)	0.40 × 0.20 × 0.08	0.30 × 0.25 × 0.20	0.50 × 0.10 × 0.07
Data collection			
Diffractometer	Siemens area detector	Siemens area detector	Siemens area detector
Data collection method	ω scans	ω scans	ω scans
Absorption correction	Multi-scan (based on symmetry-related measurements)	Multi-scan (based on symmetry-related measurements)	Multi-scan (based on symmetry-related measurements)
T_{min}	0.105	0.121	0.47
T_{max}	0.440	0.237	0.60
No. of measured, independent and observed reflections	8883, 3510, 2975	10 284, 3930, 3102	16 090, 3931, 3587
Criterion for observed reflections	$I > 2\sigma(I)$	$I > 2\sigma(I)$	$I > 2\sigma(I)$
R_{int}	0.042	0.038	0.038
θ_{max} (°)	27.5	27.0	27.5
Range of h, k, l	$-5 \Rightarrow h \Rightarrow 5$ $-16 \Rightarrow k \Rightarrow 16$ $-20 \Rightarrow l \Rightarrow 20$	$-11 \Rightarrow h \Rightarrow 11$ $-12 \Rightarrow k \Rightarrow 12$ $-17 \Rightarrow l \Rightarrow 18$	$-20 \Rightarrow h \Rightarrow 20$ $-15 \Rightarrow k \Rightarrow 15$ $-10 \Rightarrow l \Rightarrow 10$
Refinement			
Refinement on	F^2	F^2	F^2
$R[F^2 > 2\sigma(F^2)]$, $wR(F^2)$, S	0.047, 0.120, 1.09	0.050, 0.099, 1.14	0.020, 0.046, 1.04
No. of reflections	3510	3930	3936
No. of parameters	200	334	200
H-atom treatment	Constrained to parent site	Constrained to parent site	Constrained to parent site
Weighting scheme	$w = 1/[\sigma^2(F_o^2) + (0.066P)^2 + 0.42P]$, where $P = (F_o^2 + 2F_c^2)/3$	$w = 1/[\sigma^2(F_o^2) + (0.031P)^2 + 5.03P]$, where $P = (F_o^2 + 2F_c^2)/3$	$w = 1/[\sigma^2(F_o^2) + (0.014P)^2 + 1.59P]$, where $P = (F_o^2 + 2F_c^2)/3$
$(\Delta/\sigma)_{max}$	0.002	0.001	0.006
$\Delta\rho_{max}$, $\Delta\rho_{min}$ (e Å^{-3})	1.74, −1.61	1.08, −1.24	0.60, −0.54
Extinction method	None	None	*SHELXTL*
Extinction coefficient	–	–	0.00378 (9)

Computer programs used: *SMART* (Bruker, 2002), *SAINT* (Bruker, 2002), *SAINT*, *SHELXTL* (Sheldrick, 1997), *SHELXTL*.

2. Experimental

2.1. Synthesis

Chloroxynil, MCl, was obtained from Chem Service, Inc., bromoxynil, MBr, and iodoxynil, MI, were from Lancaster Synthesis, Inc. Crystals of MCl were obtained from methylene chloride, chloroform, carbon tetrachloride and acetonitrile. A crystal from carbon tetrachloride was used for the structure determination. Crystallization of MCl from benzene gave the MCl·1/2C_6H_6 complex. Crystallization of MCl from *p*-xylene gave the MCl·1/4C_8H_{10} complex.

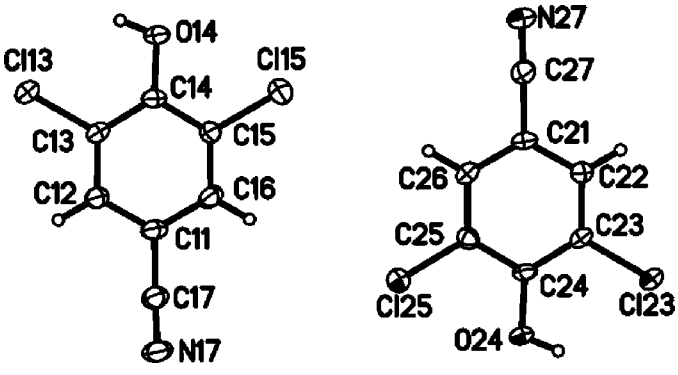

Figure 1
MCl. Displacement ellipsoids are shown at the 50% probability level.

Crystals of polymorph *A* of MBr were obtained from acetone and methanol; a crystal from methanol was used for the structure determination. Crystals of polymorph *B* were obtained from acetone, benzene, methylene chloride and acetonitrile; a crystal from acetonitrile was used for the structure determination.

Crystals of polymorph *A* of MI were obtained from carbon tetrachloride. Crystals of polymorph *C* of MI were obtained from acetone, benzene, methylene chloride and chloroform; a crystal from benzene was used for the structure determination.

2.2. Data collection, structure solution and refinement

Details of cell data, data collection and structure solution and refinement are summarized in Table 1. Absorption corrections were made using *SADABS* (Sheldrick, 1996; Blessing, 1995). The space groups of MCl-Xy and MI-*C* were assigned uniquely from the systematic absences; the rest were determined from the eventual solutions of the structures. It was intended to refine the hydroxyl H atoms, but they could not be refined meaningfully in the MI structures, so for the sake of consistency they were included at idealized position in all of the structures.

In MCl, MBr-A, MBr-B and MI-A the Z values can be described, in the notation of Zorky (1996), as $Z = 4(1^2)$. In the same notation, MI-C would have $Z = 8(1^2)$.

In the MCl·1/4 xylene structure the xylene molecules are disordered in an unusual way. They lie in channels parallel to

Table 2
Distances and angles (Å, °) in OHNC contacts.

All O—H distances are 0.84 Å.

Compound	H	N	O—H···N	H···N	H···N—C	O···N
m-Cyanophenol[a]	H9	N8	174	2.01	170	2.847 (2)
p-Cyanophenol[b]	H1*A*	N9*B*	167	1.99	174	2.82 (5)
p-Cyanophenol[b]	H1*B*	N9*A*	171	2.01	166	2.84 (5)
o-Cyanophenol[c]	H1*A*	N21*B*	173	1.96	169	2.795 (2)
o-Cyanophenol[c]	H1*B*	N21*A*	173	1.96	158	2.798 (2)
2-Hydroxy-6-(phenylmethyl)benzonitrile[d]	H21	N2	164	1.94	167	2.754 (2)
2-Hydroxy-6-(phenylmethyl)benzonitrile[d]	H22	N1	176	1.91	166	2.744 (2)
2,3-Dichloro-5,6-dicyano-1,4-dihydroxybenzene[e]	H1	N2	155	1.95	171	2.735 (3)
2,3-Dichloro-5,6-dicyano-1,4-dihydroxybenzene[e]	H2	N1	154	1.98	156	2.760 (3)
2,3-Dicyano-5,6-dichloro-4-octylphenol[f]	H1	N1	144	2.08	145	2.796 (2)
4-Amino-3,5-dicyano-2,6-diphenylphenol[g]	H1	N3	126	2.31	118	2.969 (2)
MCl	H14	N17^{i}	141	2.06	153	2.763 (3)
MCl	H24	N27^{ii}	142	2.06	152	2.771 (3)
MCl-Bz	H4	N7^{iii}	141	2.07	152	2.776 (2)
MCl-Xy	H4	N7^{iv}	145	2.05	172	2.779 (3)
MBr-*A*	H14	N27^{v}	131	2.24	101	2.867 (5)
MBr-*A*	H24	N17^{vi}	131	2.26	101	2.876 (5)
MBr-*B*	H14	N27^{v}	132	2.28	99	2.905 (6)
MBr-*B*	H24	N17^{vii}	133	2.25	100	2.889 (6)
MI-*A*	H14	N27^{v}	131	2.39	101	3.003 (9)
MI-*A*	H24	N17^{vi}	131	2.43	99	3.043 (9)
MI-*C*	H14	N17^{viii}	128	2.45	99	3.040 (7)
MI-*C*	H24	N27^{ix}	131	2.34	105	2.960 (7)

References: (*a*) Britton (2004); (*b*) Higashi & Osaki (1977); (*c*) Beswick *et al.* (1996); (*d*) Tandel *et al.* (2000); (*e*) Hoshina *et al.* (1999); (*f*) Reddy *et al.* (1993); (*g*) Tafeenko *et al.* (1994). Symmetry codes: (i) $x, -1+y, z$; (ii) $x, 1+y, z$; (iii) $1+x, y, -1+z$; (iv) $\frac{3}{2}+x, \frac{3}{2}-y, \frac{1}{2}+z$; (v) x, y, z; (vi) $x, -1+y, -1+z$; (vii) $2+x, -1+y, z$; (viii) $1-x, \frac{1}{2}+y, \frac{3}{2}-z$; (ix) $2-x, -\frac{1}{2}+y, \frac{1}{2}-z$.

the *a* axis, located more or less on centers of symmetry, but owing to their size they only occur in alternate cells. The *a* axis is not doubled because each column is independent of the others. Since this disorder leads to overlaps among the atoms, the xylene portion of the structure was constrained to have the bond lengths and angles found in the structure of pure xylene (Koningsvelt *et al.*, 1986).

In the final difference map for MI-A there were four peaks between 2.0 and 2.5 e Å^{-3}. These appeared to possibly arise from disorder. A second data set was collected from a different crystal and essentially gave the same peaks. These four peaks were located near C11, C17, N17, C21 C27 and N27; all six of these atoms showed unsatisfactory ADPs. The presence of an impurity was considered; a mass spectrum showed 2–3% of MCl as an impurity, but this did not lead to an explanation for the peaks nor for the poor ADPs. Consideration of the difference Fourier map and the peak heights suggested that there were two minor components in the disorder with abundances of $\sim 3\%$. Four models were found that could account for the four large difference map peaks, of which the most satisfactory one is reported. Minor component

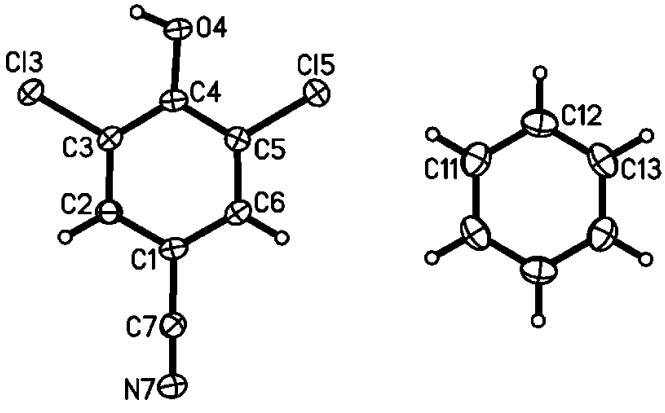

Figure 2
MCl-Bz. Displacement ellipsoids are shown at the 50% probability level. Only the independent atoms are labelled.

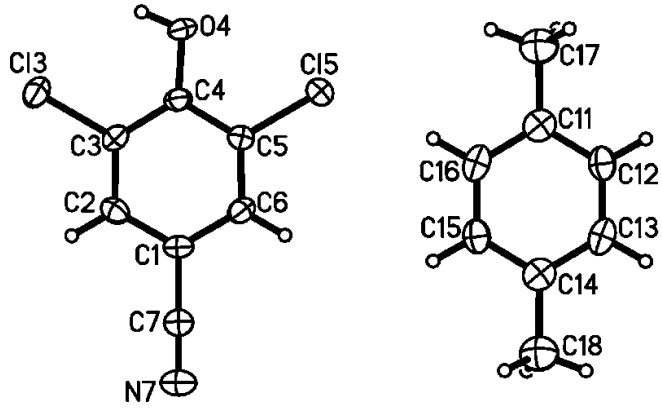

Figure 3
MCl-Xy. Displacement ellipsoids are shown at the 50% probability level. The xylene molecule was constrained to have the same bond lengths and angles as in pure xylene. The molecule was not constrained to lie on a center of symmetry, but the ADPs were constrained to be identical across the molecular center.

Table 3
Distances and angles (Å,°) in the $X\cdots X$ contacts in the layers.

For comparison, the van der Waals contact distances (Bondi, 1964) are Cl···Cl 3.50, Br···Br 3.80 and I···I 3.98 Å.

Compound	*X*1	*X*2	C1—*X*1···*X*2	*X*1···*X*2	*X*1···*X*2—C2
MCl-Bz	Cl5	Cl3^{i}	164.8 (1)	3.640 (1)	105.9 (1)
MCl-Xy	Cl3	Cl5^{ii}	167.4 (2)	3.495 (2)	150.2 (2)
MBr-*A*	Br13	Br25^{iii}	168.8 (2)	3.743 (3)	115.0 (2)
MBr-*A*	Br23	Br15^{iv}	172.9 (2)	3.711 (3)	113.0 (2)
MBr-*A*	Br15	Br23^{v}	148.2 (2)	4.099 (3)	94.6 (2)
MBr-*A*	Br25	Br13^{vi}	148.8 (2)	4.084 (3)	93.8 (2)
MBr-*B*	Br13	Br25^{vii}	172.1 (3)	3.655 (4)	111.4 (3)
MBr-*B*	Nr23	Br15^{viii}	167.8 (3)	3.751 (4)	112.0 (3)
MBr-*B*	Br15	Br23^{v}	146.6 (3)	4.152 (4)	94.2 (3)
MBr-*B*	Br25	Br13^{ix}	148.0 (3)	4.115 (4)	94.9 (3)
MI-*A*	I13	I25^{iii}	171.6 (3)	3.759 (3)	115.5 (3)
MI-*A*	I23	I15^{iv}	172.3 (3)	3.748 (3)	114.0 (3)
MI-*A*	I15	I23^{v}	150.3 (3)	4.041 (4)	92.7 (3)
MI-*A*	I25	I13^{vi}	150.6 (3)	4.022 (4)	93.1 (3)
MI-*C*	I13	I25^{v}	170.5 (3)	3.728 (2)	113.8 (3)
MI-*C*	I23	I15^{x}	176.7 (3)	3.766 (2)	113.4 (3)
MI-*C*	I15	I13^{xi}	151.3 (3)	3.999 (2)	93.1 (3)
MI-*C*	I25	I23^{xii}	150.2 (3)	4.012 (2)	94.2 (3)

Symmetry codes: (i) $x,-1+y,z$; (ii) $\frac{5}{2}-x,-\frac{1}{2}+y,\frac{3}{2}-z$; (iii) $-x,1-y,-z$; (iv) $1-x,-y,1-z$; (v) x,y,z; (vi) $x,-1+y,-1+z$; (vii) $-1+x,1-y,-z$; (viii) $2-x,1-y,1-z$; (ix) $2+x,-1+y,z$; (x) $1+x,y,-1+z$; (xi) $1-x,\frac{1}{2}+y,\frac{3}{2}-z$; (xii) $2-x,-\frac{1}{2}+y,\frac{1}{2}-z$.

A, occupancy 2.07 (10)%, is translated by *ca* [0, 0.30, 0.30] from the major component, and minor component *B*, occupancy 2.25 (12)%, by *ca* [0, −0.26, −0.26] (for a view of the minor components, see Fig. 6). Although the occupancies of the two minor components are the same within experimental error, there appears to be no reason why they should be. This disorder has been ignored in the following discussion of the packing. There was no suggestion of similar disorder either in MBr-A or in MI-C.

3. Results and discussion

3.1. Molecular structures

Figs 1–7 show the atom labelling and anisotropic displacement ellipsoids for all the independent molecules. All the bond distances and angles are normal. The distortions of the ring angles from 120° are in reasonable agreement with the substituent effects described by Domenicano (1992). Also, in every case the exocyclic angles at the C4 atoms are larger on the side *cis* to the OH bond than on the *trans* side. This is commonly the case in phenols and appears to be a consequence of crowding of the OH hydrogen atom.

Table 4
Unit-cell dimensions (Å, °) after converting the cells so that the revised cells have the molecular planes parallel to (001).

The matrices to convert the cells in Table 1 to these cells: MBr-*A* and MI-*A*, 0,−1,−1/1,−1,1/−1,0,0; MBr-*B*, 2,−1,0/1,0,−1/−1,0,0; MI-*C*, 0,1,0/−1,0,1,0,0,1.

Compound	*a*′	*b*′	*c*′	*α*′	*β*′	*γ*′
MBr-*A*	14.105 (4)	17.000 (4)	9.120 (2)	42.41 (1)	55.55 (1)	90.45 (1)
MBr-*B*	14.114 (4)	16.996 (4)	3.968 (1)	109.71 (1)	116.99 (1)	89.37 (1)
MI-*A*	14.357 (4)	17.646 (4)	9.393 (2)	41.28 (1)	56.86 (1)	90.28 (1)
MI-*C*	14.320 (4)	17.606 (4)	7.742 (2)	62.10 (1)	90	90

3.2. Packing and intermolecular interactions

3.2.1. General. In all of the structures there are O—H···N—C hydrogen bonds. The metric data for these bonds are given in Table 2. In most of the structures there are significant $X\cdots X$ contacts. Metric data for these are given in Table 3. Finally, in the MBr and MI structures there is two-dimensional isostructurality. The metric data comparing this isostructurality are given in Table 4.

3.2.2. MCl. The packing of MCl is shown in Fig. 8. The O—H···N—C hydrogen bonds lead to chains of molecules parallel to **b**. The chains form layers parallel to (100). The two independent molecules are tilted with respect to (100), molecule 1 by 33.1 (1) and molecule 2 by 6.1 (1)°; the angle between the planes of the two molecules is 39.2 (1)°.

The attractions between the central chains in Fig. 8 involve eight-membered rings with two Cl···O contacts in each ring. The attraction between the top two chains involves eight-membered rings with two H···Cl contacts in each ring. None of these contacts has a distance less than the usual van der Waals distance. There are no Cl···Cl contacts within the layers shorter than 4.0 Å. There are four independent Cl···Cl

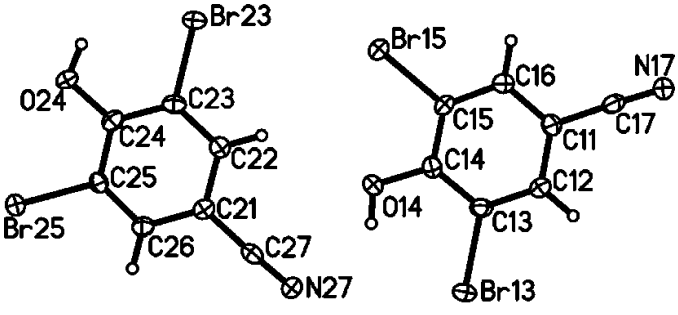

Figure 4
MBr-*A*. Displacement ellipsoids are shown at the 50% probability level. In Figs. 4–7 the molecules are shown in their correct juxtaposition; they are connected by an O—H···N—C hydrogen bond.

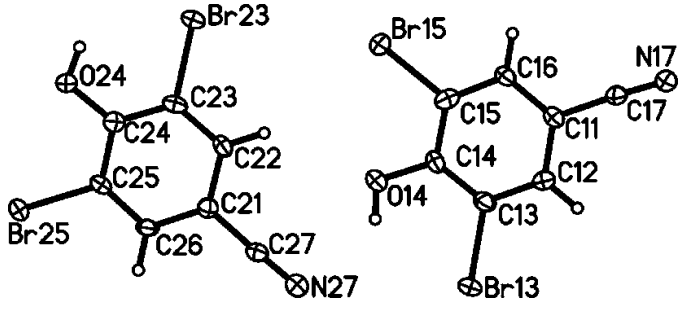

Figure 5
MBr-*B*. Displacement ellipsoids are shown at the 50% probability level.

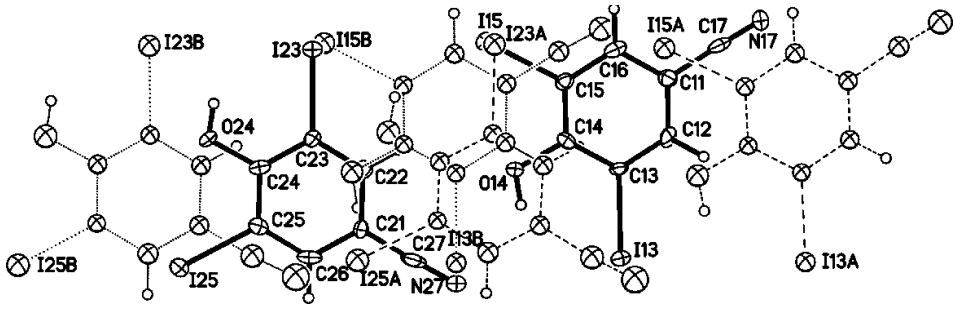

Figure 6
MI-*A*. Displacement ellipsoids are shown at the 50% probability level. The two minor components of the disorder are shown with dashed and dotted bonds. (See text for details of the disorder.)

contacts between the layers with distances bewteen 3.6 and 4.0 Å.

3.2.3. MCl-Bz. The packing of MCl-Bz is shown in Fig. 9. Again there are chains of molecules joined by OH···NC hydrogen bonds, lying along the [1,0,−1] direction. The chains form layers parallel to (101). The molecules are tilted with respect to (101) by 3.4 (1)°. Adjacent chains are held together by Cl···Cl 3.640 (1) Å contacts (see Table 3). There is a Cl···Cl contact between layers of 3.653 (1) Å and two others between 4.0 and 4.5 Å. The benzene molecules lie in pockets between alternate pairs of MCl layers.

3.2.4. MCl-Xy. The packing of MCl-Xy is shown in Fig. 10. Again there are chains of molecules joined by OH···NC hydrogen bonds, lying along the [301] direction. The chains form layers parallel to (1,0,−3). The molecules are tilted with respect to (1,0,−3) by 39.8 (1)°. Adjacent chains are held together by Cl···Cl 3.495 (2) Å contacts. There are two Cl···Cl contacts between layers between 3.7 and 3.9 Å. The xylene molecules lie in channels through the layers parallel to **a**. The size of the xylene molecule is such that there is only one for every two layers. That is, if there is a molecule centered at $\frac{1}{2},\frac{1}{2},\frac{1}{2}$, as shown in Fig. 10, there will not be one at $\frac{3}{2},\frac{1}{2},\frac{1}{2}$, but there will be at $\frac{5}{2},\frac{1}{2},\frac{1}{2}$. If the xylene were completely ordered, this would lead to a doubling of **a**, but the channels are independent of each other and the xylenes are disordered between two origins in each channel.

3.2.5. MBr-*A*, MBr-*B*, MI-*A* and MI-*C*. The packing of MBr-*A* and MI-*A* is shown in Fig. 11, of MBr-*B* in Fig. 12 and of MI-*C* in Fig. 13. As can be seen, there are two-dimensional layers in all of these structures that are virtually the same. In all four the OH···NC contacts are further from linear than those found in the three MCl structures. In all four there are fairly short *X*···*X* contacts between the chains and longer ones within the chains; both types are included in Table 3.

In the isostructural pair, MBr-*A* and MI-*A*, the two crystallographically independent molecules alternate in each chain. Layers are parallel to (2,1,−1) with molecular tilts of 5.4 (1) and 1.5 (1)° in MBr-*A*, and 2.9 (1) and 2.7 (1)° in MI-*A*; the angle between the planes of the molecules is 5.0 (1)° on MBr-*A* and 0.2 (1)° in MI-*A*. In MBr-*A* there are eight crystallographically independent interlayer Br···Br contacts between 3.9 and 4.3 Å. In MI-*A* there are nine crystallographically independent interlayer I···I contacts between 4.1 and 4.5 Å.

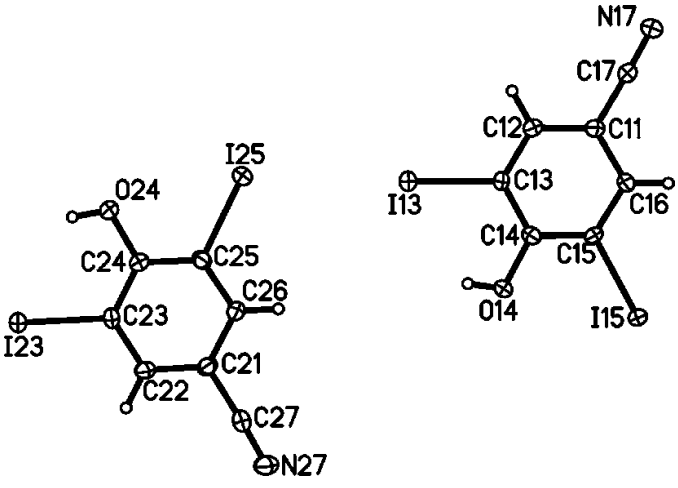

Figure 7
MI-*C*. Displacement ellipsoids are shown at the 50% probability level. In this polymorph each molecule forms O—H···N—C hydrogen bonds with crystallographically equivalent molecules.

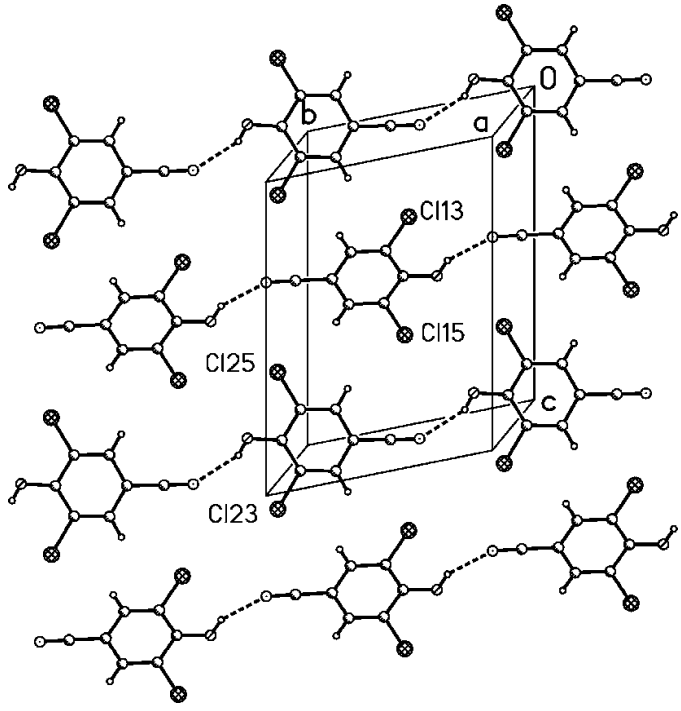

Figure 8
The packing of MCl. View normal to (100). The O—H···NC contacts are shown as double dashed lines here and in Figs. 9–13.

In MBr-*B* (Fig. 12) the two crystallographically independent molecules alternate in each chain. Layers are parallel to (1,2,−1) with molecular tilts of 7.0 (1) and 4.3 (1)°; the angle between the planes of the molecules is 2.8 (1)°. There are 13 crystallographically independent interlayer Br···Br contacts between 3.9 and 4.3 Å.

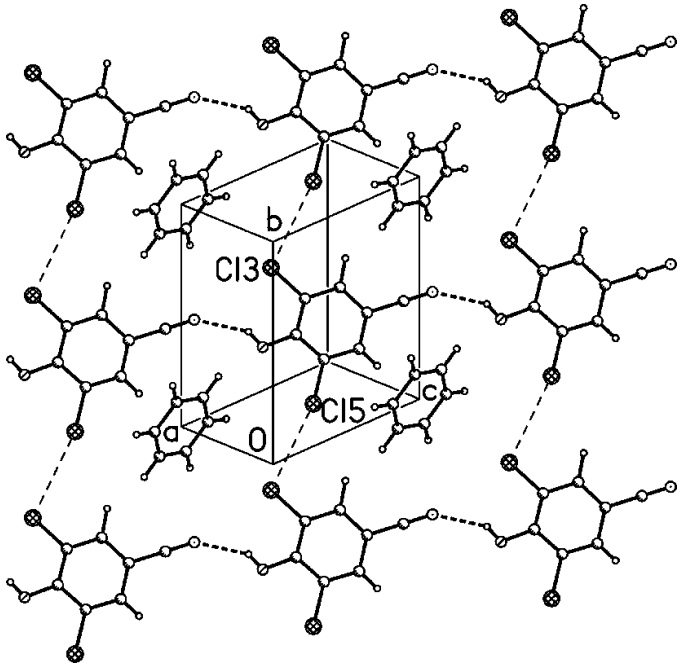

Figure 9
The packing of MCl-Bz. View normal to (101). The dashed lines show Cl···Cl contacts of 3.640 (1) Å.

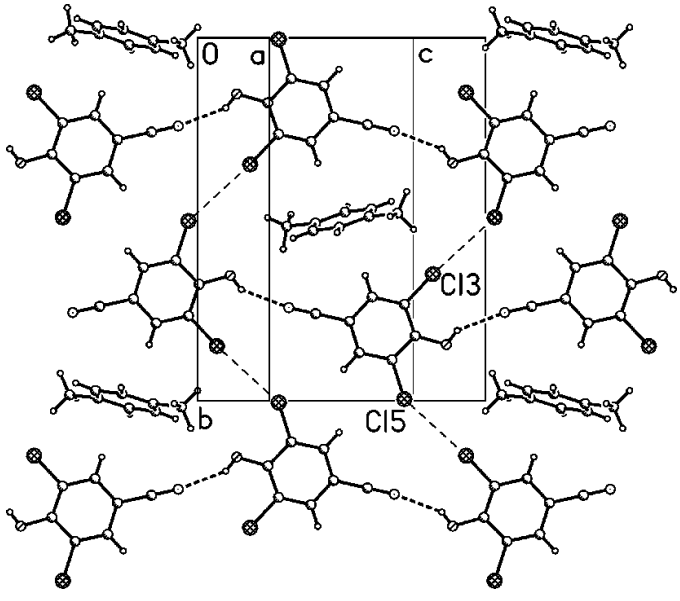

Figure 10
The packing of MCl-Xy. View normal to (1,0,−3). The dashed lines show Cl···Cl contacts of 3.495 (2) Å. The xylene molecules are shown at one of two disordered positions.

In MI-*C* (Fig. 13), each chain consists of one type of molecule and alternate chains are crystallographically independent. Layers are parallel to (101) with molecular tilts of 3.5 (1) and 1.0 (1)°; the angle between the planes of the molecules is 3.1 (1)°. There are eight crystallographically independent interlayer I···I contacts between 4.1 and 4.5 Å.

3.2.6. OH···NC interactions. The OH···NC contacts are similar in all the compounds with the graph-set *C*(7) (Etter *et al.*, 1990). However, the geometries of the contacts are different, with OH···H angles of 142 ± 1° for the MCl

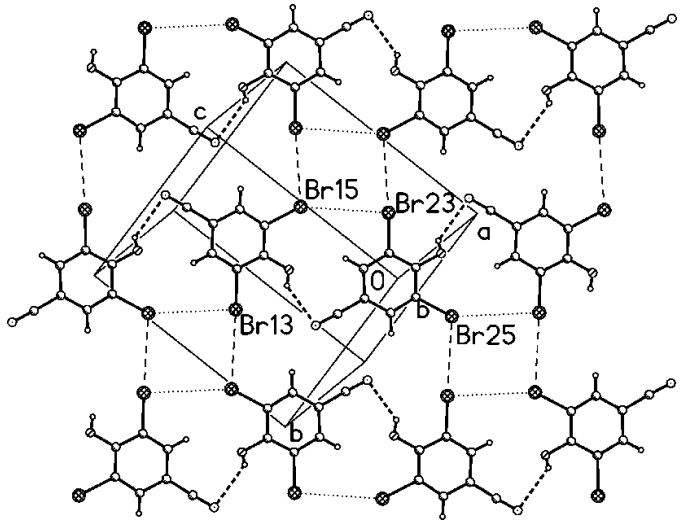

Figure 11
One layer of MBr-*A*. View normal to (2,1,−1). The dashed bonds show Br···Br contacts of 3.711 (3) and 3.743 (3) Å. The dotted lines show Br···Br contacts of 4.084 (3) and 4.095 (3) Å. A layer of MI-*A* would be virtually the same with I···I contacts of 3.748 (3), 3.759 (3), 4.022 (4) and 4.041 (4) Å.

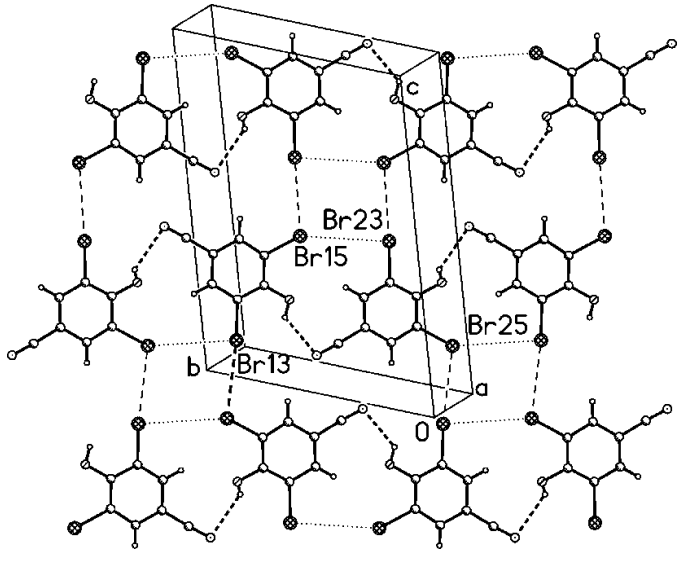

Figure 12
One layer of MBr-*B*. View normal to (1,2,−1). The shorter (dashed) Br···Br distances are 3.655 (4) and 3.751 (4) Å. The longer (dotted) distances are 4.115 (4) and 4.152 (4) Å.

structures and 131 ± 1° for the MBr and MI structures; the corresponding H···NC angles are 157 ± 7° and 102 ± 3°. The metric details of these contacts are given in Table 2, where they are compared with similar contacts in other cyanophenols. In each case the O—H distance has been adjusted to 0.84 Å for the sake of comparison. The ideal geometry for an OH···NC contact would be expected to be linear at both H and N. It can be seen in all of the compounds that approximately this geometry is found. It can also be seen that the greater the deviations from linearity at H and N the longer the H···N distance and, presumably, the weaker the interaction. Table 2 is roughly ordered from the most linear to the least linear contacts. As can be seen in Table 2, the contacts become weaker (longer) from Cl to Br to I. This is probably a consequence of the $X\cdots X$ interactions becoming stronger, although inductive effects from the *ortho* halogen atoms may be making the hydroxyl H atoms more positive in MCl than in MBr than in MI.

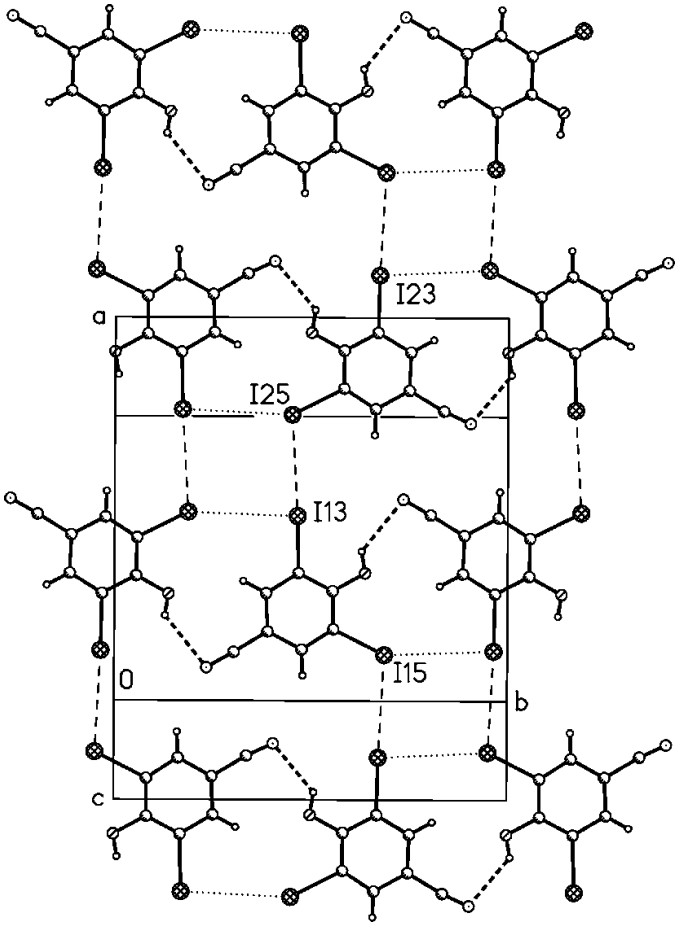

Figure 13
One layer of MI-*C*. View normal to (101). The shorter (dashed) I···I distances are 3.733 (2) and 3.773 (2) Å. The longer (dotted) distances are 3.988 (2) and 4.000 (2) Å.

3.2.7. Halogen–halogen interactions. The distances and angles in the various $X\cdots X$ contacts are all within the range found in previously reported structures. These interactions have been discussed by Desiraju (1989), who supports the view that at least in some instances such contacts can be regarded as weak Lewis acid–base (or electron acceptor–donor) interactions. This view was put forth by Bent (1968) for $X\cdots X$ contacts, inspired in part by the ground-breaking work of Hassel (see, for example, Hassel & Romming, 1962) in which such interactions were unmistakeably shown in a series of co-crystals involving $X\cdots$N and $X\cdots$O contacts.

In the series of compounds reported here it appears that the Cl···Cl interactions are not strong enough to determine the main features of the structures, while with Br and I the $X\cdots X$ interactions are stronger and lead to the two-dimensional isostructuality that is found in these structures.

3.2.8. Stacking. Although the π-stacking interactions are essential to the structures, there do not appear to be any unusual stacking features. There are 11 crystallographically independent species in this series of structures, with 22 contacts between benzene rings and molecules in the next layer. Of these, only four involve ring-to-ring overlap, seven involve ring hydrogen-to-ring overlap, seven involve halogen-to-ring overlap, four involve nitrile-to-ring overlap, and one involves oxygen-to-ring overlap. As part of the comparison of the MBr and MI isomorphs, the stacking in these structures is shown in the next section.

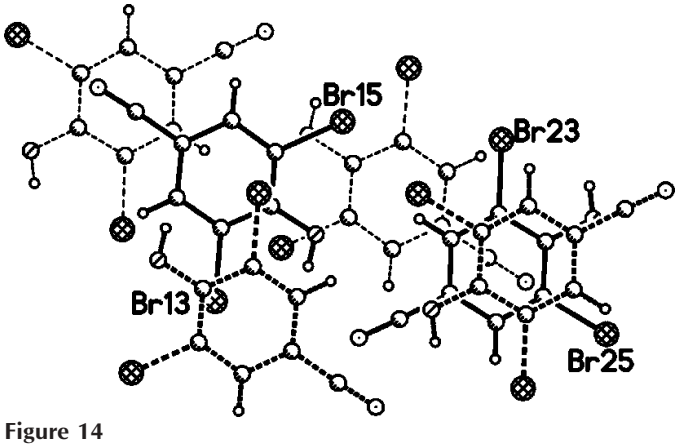

Figure 14
Layer stacking in MBr-*A* (and MI-*A*, major component). The molecules with solid bonds are those shown in Fig. 11; those with heavy dashed bonds are in the layer above; those with light dashed bonds are in the layer below.

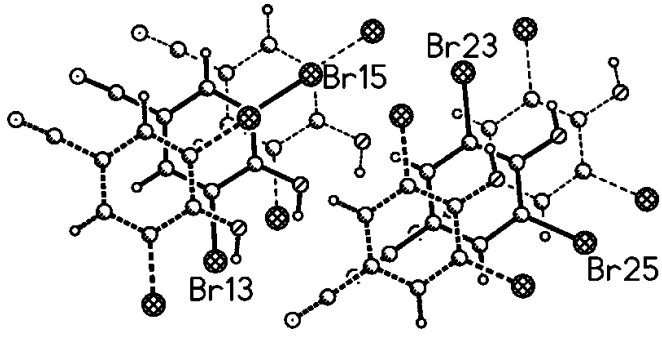

Figure 15
Layer stacking in MBr-*B*. Conventions as in Fig. 14. Central molecules as shown in Fig. 12.

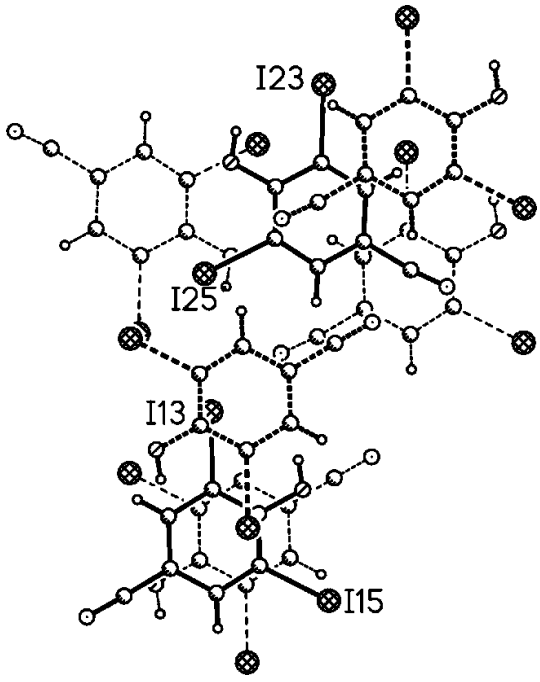

Figure 16
Layer stacking in MI-*C*. Conventions as in Fig. 9. Central molecules as shown in Fig. 13.

3.3. General discussion of the MBr and MI structures

As mentioned above, the layers in the four MBr and MI structures are essentially the same. They all approximate a two-dimensional *p2gg* arrangement. If the unit cells are redefined so that a' is horizontal and b' is vertical in Figs. 11, 12 and 13, the cells given in Table 4 are obtained. The γ' angles are all near 90°, although the differences from 90° are greater than the s.u.s in the *A* and *B* polymorphs. In the *A* and *B* forms both glides are pseudo-symmetry elements. In the *C* form only the longer of the two glide axes is a pseudo-axis; as a consequence, γ' is exactly 90° in this form.

The differences among the polymorphs are in the stacking of the layers. Three successive layers of MBr-*A*, MBr-*B* and MI-*C* are given in Figs. 14, 15 and 16, respectively. It can be seen that the stacking sequences in the three polymorphs, while having some points of similarity, are distinctly different. It can also be seen that in each case the stacking at molecule 1 is different from that at molecule 2.

Structures in which the same two-dimensional arrangements occur in different three-dimensional polymorphs are not new. For example, 4,5-dichloro- and 4,5-dibromobenzofurazan-1-oxide both occur in two polymorphs with similar layers and different stacking arrangements (Ojala *et al.*, 1999; Britton *et al.*, 2003). The general concept has recently been discussed by Fábián & Kálmán, 2004).

Finally, it should be noted that while MBr-*C* and MI-*B* have not been found they are distinct possibilities.

References

Baughman, R. G., Virant, M. S. & Jacobson, R. A. (1981). *J. Agric. Food Chem.* **29**, 989–991.
Bent, H. A. (1968). *Chem. Rev.* **68**, 587–648.
Beswick, J., Davis, R. E., Shimoni, L. & Chang, N.-L. (1996). *Angew. Chem. Int. Ed. Engl.* **34**, 1555–1573.
Blessing, R. H. (1995). *Acta Cryst.* A**51**, 33–38.
Bondi, A. (1964). *J. Phys. Chem.* **68**, 441–451.
Britton, D. (2000). *Acta Cryst.* B**56**, 828–832.
Britton, D. (2004). *Acta Cryst.* E**60**, o1513–o1514.
Britton, D., Noland, W. E., Pinnow. M. J. & Young Jr, V. G. (2003). *Helv. Chim. Acta*, **86**, 1175–1192.
Bruker (2002). *SMART and SAINT*. Bruker AXS Inc., Madison, Wisconsin, USA.
Domenicano, A. (1992). *Accurate Molecular Structures*, edited by A. Domenicano & I. Hargittai, pp. 437–468. Oxford University Press.
Desiraju, G. R. (1989). *Crystal Engineering; the Design of Organic Solids*, pp. 175–201. Amsterdam: Elsevier.
Etter, M. C., MacDonald, J. C. & Bernstein, J. (1990). *Acta Cryst.* B**46**, 256–262.
Fábián, L. & Kálmán, A. (2004). *Acta Cryst.* B**60**, 547–558.
Hassel, O. & Romming, C. (1962). *Q. Rev.* **16**, 1–18.
Higashi, T. & Osaki, K. (1977). *Acta Cryst.* B**33**, 607–609.
Hoshina, G., Ohba, S. & Tsuchimoto, M. (1999). *Acta Cryst.* C**55**, 592–594.
Koningsveld, H. van, Berg, A. J. van den, Jansen, J. C. & Goede, R. de (1986). *Acta Cryst.* B**42**, 491–497.
Ojala, C. R., Ojala, W. H., Britton, D. & Gougoutas, J. Z. (1999). *Acta Cryst.* B**55**, 530–542.
Reddy, D. S., Paneerselvam, K., Pilati, T. & Desiraju G. R. (1993). *Chem Commun.* pp. 661–662.
Sheldrick, G. M. (1996). *SADABS*. University of Göttingen, Germany.
Sheldrick, G. M. (1997). *SHELXTL*, Version 5. Siemens Analytical X-ray Instruments Inc., Madison, Wisconsin, USA.
Tafeenko, V. A., Bogdan, T. V. & Aslanov, L. A. (1994). *J. Struct. Chem.* **35**, 562–567.
Tandel, S., Hongming, Z., Qadri, N., Ford, G. P. & Biehl, E. R. (2000). *J. Chem. Soc. Perkin Trans. 1*, pp. 587–589.
Zorky, P. M. (1996). *J. Mol. Struct.* **374**, 9–28.